Version of Record: https://www.sciencedirect.com/science/article/pii/S0169555X20302567
Manuscript_4235bd01e1fa2de1d077bc59407492dd

A 5200-year Paleoecological and Geochemical Record of Coastal Environmental Changes and Shoreline Fluctuations in Southwestern Louisiana: Implications for Coastal Sustainability

Qiang Yao[1]*, Kam-biu Liu[1], Alejandro Antonio Aragón-Moreno[1], Erika Rodrigues[2], Y. Jun Xu[3], Nina S. Lam[4],

[1] Department of Oceanography and Coastal Sciences, College of the Coast and Environment, Louisiana State University, Baton Rouge, LA 70803

[2] Laboratory of Coastal Dynamics, Graduate Program of Geology and Geochemistry, Brazil Federal University of Pará, Belém (PA), Brazil.

[3] School of Renewable Natural Resources, Louisiana State University, Baton Rouge, LA 70803

[4] Department of Environmental Sciences, Louisiana State University, Baton Rouge, LA 70803

*Corresponding author:

Qiang Yao

Department of Oceanography and Coastal Sciences, Louisiana State University, 93 South Quad Drive, Baton Rouge, LA 70803

qyao4@lsu.edu

Highlights:

- Louisiana's Chenier Plain was strongly influenced by the Mississippi-Atchafalaya River course changes.
- Coastal ecosystems changed from swamp to maritime forest during 5200-3440 cal yr BP, and from swamp to marsh to beach/dune community after 3440 cal yr BP.
- Shoreline retrogradation began at ~3440 cal yr BP as the Mississippi River outlet switched from west to east.
- Holocene shoreline fluctuations of the Chenier Plain were tied to the Mississippi River Delta Switch and relative sea level rise.

Keywords: Coastal morphodynamics, Palynology, Shoreline fluctuations, Mississippi River Delta Switch, Louisiana Chenier Plain, Holocene

1. Introduction

Coastal wetlands provide many essential ecological services to coastal communities. Particularly, in the state of Louisiana, wetlands are a vital natural resource because Louisiana has the largest contiguous wetland system in the lower 48 states and contains over 40% of the wetlands in the continental U.S. (Couvillion and Beck, 2013). However, since the 1930s, almost 5000 km^2 of wetlands have disappeared from the Louisiana coastlines, accounting for ~90% of the total coastal wetland loss in the continental U.S. (Couvillion et al., 2011, 2017). Particularly during the peak of wetland loss between 1970s and 1980s, an area of wetlands equivalent to the size of a football field disappeared every hour (Couvillion et al., 2011). This rapid wetland loss is caused by a combination of human and natural processes, such as hydrology alteration, landscape fragmentation, coastal excavation, subsidence, sea level rise, and hurricanes (Bush et al., 2018; Lam et al., 2018a, b; Schoolmaster et al., 2018; Xu et al., 2018). Among them, the Mississippi River Delta Switch is believed to play an important role in the chronic wetland loss in Louisiana (Roberts, 1997) because the substrate of both western and eastern Louisiana coastlines was formed from sediments deposited and carried by the Mississippi River over the past 7000 years (Rosen and Xu, 2011). For every ~1000 years, the Mississippi River changed its course and caused erosion, compaction, and subsidence to the old delta lobe, subsequently reshaping the coastal morphodynamics and ecosystem development in Louisiana (Roberts, 1997; McBride et al., 2007; Owen, 2008; Rosen and Xu, 2011) (Fig. 1). During the past few decades, these natural deltaic cycles have been heavily altered by human activities, accelerating the deterioration of coastal ecosystems - an estimated net loss of 1,700 km^2 of coastal wetlands in Louisiana by 2050 (Reed and Wilson, 2004). Thus, to predict the coastal morphodynamics and ecosystem development in the future, it is essential to reveal the history of coastal wetland development in relation to the delta switch in Louisiana since the mid-Holocene.

During recent decades, the cyclic delta-building process of the Mississippi River has been documented in a number of studies (Coleman, 1988; Roberts, 1997; Coleman et al., 1998). It is generally acknowledged that six major delta complexes (Sale-Cypremont 4600-3500 BP, Teche ~3500-2800 BP, St. Bernard ~2800-1000 BP, Lafourche ~1000-300 BP, Plaquemine-Balize 750 BP to present, Atchafalaya-Wax Lake 400 BP to present) were developed since the mid-Holocene (Roberts, 1997; Day et al., 2007; McBride et al., 2007; Kemp et al., 2016) (Fig. 1). These deltaic cycles significantly influenced the geomorphology of the Louisiana Chenier Plain, an extension of the Mississippi Deltaic Plain. The Louisiana Chenier Plain is one of the world's largest chenier plains (Schwartz, 2006) comprising an area of about 5000 km^2 with a west-east coastline of approximately 200 km stretching from approximately 29.5º N to 33.2º N and from 91.3º W to 94.0 º W (He and Xu, 2016). Previous studies have suggested that when the Mississippi River delta complex switched to a relatively western position (Sale-Cypremont and Atchafalaya-Wax Lake), the southwestern Louisiana coastlines underwent coastal progradation from renewed sediment input from the Mississippi River, forming the foundation of coastal wetlands in southwestern Louisiana (Owen, 2008). When the complex switched to farther east (Teche, St. Bernard, Lafourche, Plaquemine/Balize), coastlines experienced retrogradation and cheniers were formed because marine processes overwhelmed fluvial processes (McBride et al., 2007). Although these studies provided background datasets to study the Holocene geomorphological history of Louisiana coastlines, major gaps still exist in the paleoecological data network – the Holocene history of coastal wetland development in southwestern Louisiana has not been documented. In particular, the link between the Mississippi River Delta Switch and the southwestern Louisiana coastal morphodynamics is still unclear (Rosen and Xu, 2011).

Since the mid-Holocene, a dense layer of fluvial sediments and humic clay has deposited on the wetlands in Louisiana's Chenier Plain (Roberts, 1997; Owen, 2008), providing an ideal repository for proxy-based paleoecological, hydrological, and sedimentological reconstructions. Among different proxy methods, palynological analysis has been widely used for the reconstruction of vegetation and ecosystem development in North America (e.g., Huntley and Webb, 2012). However, well-dated palynological records are remarkably rare from coastal areas in the continental U.S. (Willard et al., 2001, 2004; Willard and Bernhardt, 2011; Van Soelen et al., 2012; Yao et al., 2015; Yao and Liu, 2018, 2017; Jones et al., 2019), and even fewer studies have documented the wetland development in Louisiana at centennial to millennial timescales (Ryu et al., 2018; Kiage, 2020). Chenier Plains are investigated in many coastal regions for their marine influences. Very little is known about the long-term impacts of alluvial sediments from the near-by rivers on chenier shoreline development and the ecosystem changes associated with it.

To fill the knowledge gap, this study utilizes a multi-proxy approach to reconstruct the sedimentary history of the Louisiana Chenier Plain and investigates chenier ecosystem changes associated with it. Our goal was to test the hypotheses that 1) the morphodynamic development of the Louisiana Chenier Plain is dominated by the Mississippi River, and 2) changes in the course and sediment supply of the Mississippi River will therefore strongly affect the physical and ecosystem development of the Chenier Plain. Specially, the study used palynological, loss-on ignition (LOI), grain-size, and X-ray fluorescence (XRF) measurements of a 525 cm sediment core (ROC-4) from the Chenier Plain at Rockefeller Wildlife Refuge (RWR) (Fig. 1) to reconstruct the Holocene history of coastal wetland development on the southwestern Louisiana coastlines in relation to the Mississippi River Delta Switch on a regional scale. The study also employed hydrologic and remote sensing data to assess the recent development of the chenier ecosystem in light of future coastal morphodynamics and restoration strategies.

2. Research area

2.1. Study Site Description

Our study area, Rockefeller Wildlife Refuge (RWR), is a state-owned large area of marshland located at the eastern end of the Chenier Plain in Cameron and Vermillion parishes, southwestern Louisiana (Fig. 1). The RWR sits on a narrow basin with low beach barriers to the south and high ridges to the north. Before the occurrence of major landscape alterations due to human activities, precipitation and fluvial discharge from surrounding ridges drain into this basin, thus creating extensive freshwater marshes near the north side of RWR (Selman et al., 2011). Vegetation in the freshwater marsh is primarily comprised of cattail (*Typha* sp.), grasses (*Poa* sp.), and sawgrass (*Cladium* sp.). The lower two-thirds of the basin are drained by dendritic tidal channels, thus inhabiting brackish marsh in the middle of the basin and saltmarsh close to the beach. Vegetation in the lower two-thirds of the basin are dominated by *Spartina* sp., with wiregrass (*Spartina patens*) dominating the brackish marsh and iva (*Iva frutescens*), hogcane (*Spartina cynosuroides*), and cordgrass (*Spartina alterniflora*) dominating the saltmarsh (Selman et al., 2011). At the south end of RWR are beaches consisting of shells and shell fragments that become coarser landward from the shoreline (Selman et al., 2011). Some foraminifera, and few quartz and gravels fragments are also present along the beach (Yao et al., 2018). *Batis maritima*, a succulent plant commonly found in saltmarshes and beach ridges along the Gulf coastlines, occupies extensive backbarrier marshes behind the beach. The vegetation composition of the natural wetlands in RWR has been altered substantially over the past 40 years due to water management and construction of levees and infrastructures (Selman et al., 2011). A recent study indicates that the shoreline in RWR was retreating at a rate of ~14.5 cm/yr since 1998 (Yao et al., 2018). Therefore, there is an urgent need to document the Holocene history of these coastal wetlands before they are lost to shoreline retreat and coastal erosion.

2.2. The Holocene history of the Mississippi River Delta complexes

The framework of the Mississippi River Delta cycle was established in the early 1950s by McIntire (1954). Based on McIntire's initial concept, the first widely used delta complexes diagram was published in the late 1950s by Kolb and Van Lopik (1958). Later on, the chronology of different complexes was established in the 1960s (McFarlan, 1961; Frazier, 1967). In recent decades, the framework and chronology of the Delta complex-building processes have been improved and reviewed by several landmark studies (Coleman, 1988; Coleman et al., 1998; 2007; Kemp et al., 2016). Since the timeline of the delta cycle is defined slightly differently by various authors, this study attempts to synthesize the Holocene history of the Mississippi River Delta complexes based on the commonly cited studies published in recent years (Roberts, 1997; Day et al., 2007; McBride et al., 2007; Kemp et al., 2016;). Our synthesis recognizes six phases in the development of the Mississippi River Delta complexes: (1) Sale-Cypremont (4600-3500 BP), (2) Teche (3500-2800 BP), (3) St. Bernard (2800-1000 BP), (4) Lafourche (1000-300 BP), (5) Plaquemine-Balize (750 BP to present), and (6) Atchafalaya-Wax Lake (400 BP to present) (Roberts, 1997; Day et al., 2007; McBride et al., 2007; Kemp et al., 2016) (Fig. 1). These complexes typically turned-around at a frequency of every ~1000-2000 years, deposited sedimentary profiles up to 300 cm thick on the inner shelf (Roberts, 1997).

3. Materials and methods

3.1 Field sampling

In 2013, a 525 cm sediment core ROC-4 (29.668935°N, 92.850490°W) was recovered from the succulent marsh ~30 meter behind the beach barrier in RWR. The elevation of the coring site was ~1 m above the sea-level at the of time of coring but submerged after 2017 due to rapid shoreline retreat. The core was retrieved by using a Russian peat borer and consisted of eleven ~50 cm-long core segments. Each of the core segment was measured, photographed, and wrapped in the field, and stored in a cold room (4°C) at the Global Change and Coastal Paleoecology Laboratory in Louisiana State University.

3.2 Laboratory analyses

In this study, grain-size analysis was performed at contiguous 20 cm interval throughout core ROC-4 by using a Malvern Mastersizer 2000 grainsize analyzer. Approximately 1 gram (dry weight) of sediments was used for each sample, and the laboratory procedures followed the standard protocols described in Zhang et al. (2019). Accordingly, the sand (63-2000 μm), silt (2-63 μm), and clay (< 2 μm) fractions were reported for each sample.

Loss-on-ignition (LOI) and X-ray fluorescence (XRF) analyses were performed at contiguous 1 cm interval throughout the core. LOI analysis reveals the % wet weight for water, and % dry weight for organics and carbonates in the sediment profile (Liu and Fearn, 2000). XRF analysis was performed by using an Olympus Innov-X DELTA Premium XRF analyzer. XRF is widely used in coastal studies and it measures the elemental concentrations (ppm) of major chemical elements in coastal sediments (e.g., Ca, Sr, and Zr) (Yao and Liu, 2017, 2018; Yao et al., 2018, 2019). Among the detected elements, only Ca and Sr showed significant and meaningful fluctuations throughout the core and are therefore reported here.

Thirty samples were taken at 5 to 20 cm intervals for palynological analysis. Each sample consisted of 1.8 ml of sediments. All pollen samples were processed using standard laboratory procedures described in Kiage and Liu (2009) and Yao et al. (2015). One tablet of *Lycopodium* (L_c) (~20,583 spores) was added to each sample as an exotic marker to aid the calculation of pollen concentration (grains/cm^3) (sum = Lc added ∗ no. of spores counted/Lc counted/volume of sample). Pollen identification was based on published pollen keys by Chmura et al. (2006), Willard et al. (2004), and McAndrews et al. (1973). Over 300 grains of pollen and spore were counted and photographed in every sample by using an Olympus microscope at 400x magnification. Other palynomorphs, including charcoal fragments (>10 μm in size), dinoflagellates tests, and foraminifera linings were also counted. The grain-size, LOI, XRF, and pollen results are displayed in Figure 2.

3.3 Statistical analyses

Principal component analysis (PCA) was performed to reveal the distribution of pollen taxa in relation to coastal morphodynamics and ecosystem development by using the C-2 version 1.8 (standardize data by variables, center data by variables, rotate axes) on all pollen samples. The PCA provided a foundation to categorize various pollen taxa into statistically meaningful groups, which were then used to verify wetland sub-environments interpreted from the pollen dataset.

3.4 Chronology

Three samples from core ROC-4 were sent to International Chemical Analysis Inc., Florida, for AMS ^{14}C measurements (Table 1). Approximately 1 gram of sediment was used for each ^{14}C sample. Pretreatment for each sample was performed in the Global Change and Coastal Paleoecology Laboratory at Louisiana State University by sieving the sediments with a 200 µm sieve to separate the <200 µm fine sediment fraction consisting of bulk clastic and organic sediments from the >200 µm coarse sediments fraction consisting of roots and sand (Yao et al., 2015). The fine sediment fractions were used for AMS ^{14}C measurements. More detailed information describing the pretreatment of ^{14}C samples from dynamic coastal environments is provided in supplementary content published by Yao et al. (2015). All ^{14}C dates in this study were converted into calendar years before present (BP) by Calib 7.1 (Stuiver et al., 2020), rounded to the nearest decade, and reported as calibrated year before present (cal yr BP).

4. Results

4.1 Chronology

All three AMS ^{14}C dates were deemed reliable. They were obtained at 78 cm, 403 cm, and 525 cm from the top of the core and calibrated to ~ 590, 4340, and 5190 cal yr BP after rounding to the nearest decade (Table 1). The surface (0 cm at 2013 AD) and the three ^{14}C dates were used to calculate the sedimentation rate based on linear interpolation between points. This age model suggests that the sedimentation rate from 590 cal yr BP to the present was 1.19 mm/yr; the sedimentation rate from 4340 - 590 cal yr BP was 0.88 mm/yr; and the sedimentation rate from 5190 - 4340 cal yr BP was 1.44 mm/yr (Fig. 2).

4.2 Core stratigraphy and geochemical characteristics

Core ROC-4 consists of two different types of sediments (Fig. 2). Silt-clay sediments in brownish color occur from 525 to 40 cm. The core stratigraphy and geochemical profiles show relatively stable signals throughout these brownish silt-clay sediments. The sand, silt, and clay fractions vary slightly from 0-5%, 40-50%, and 50-60 %, respectively, in this section, and the sand and silt fractions increase progressively from 150 to 40 cm. The contents of water (50-60 %), organic matter (5-15 %), and carbonates (2-5 %) and the concentrations of Ca (2000-5000 ppm) and Sr (50-100 ppm) are also consistent throughout this section. Nonetheless, a few sediment layers exhibit some variations. Grain-size data indicate that sediment intervals at 320, 280, and 100 cm have higher contents (2-5 %) of sand and silt fractions comparing with other intervals in this section. XRF data also reveal a few layers with elevated Ca and Sr contents; particularly, sediment intervals at 195-215 cm have 10 to 20 times higher concentrations of Ca (20000 to 40000 ppm) and slightly higher concentrations of Sr in relative to other intervals. In addition, some charcoal fragments, rootlets, and leaflets were also found throughout this section, but overall, the stratigraphy and geochemical datasets show stable results in this silt-clay section (Fig. 2).

Above the silt-clay section is a 40-cm layer of sediments consisting of muddy-sand, shell fragments, foraminifera, and some quartz grains and gravels (Fig. 2). Grain-size analysis shows that the sand (10-15 %) and silt (> 50 %) fractions in this section are higher than the silt-clay section beneath. In particular, the top 10 cm of core ROC consists of mainly shell fragments and foraminifera. Macroscopic analysis identified three genera of shells (*Littoraria*, *Anadara*, and *Mactridae*) and two genera of foraminifera (*Elphidium* and *Ammonia*). *Anadara* and *Mactridae* are marine bivalve mollusks, *Littoraria* belongs to a genus of sea snails, and *Elphidium* and *Ammonia* both inhabit in subtidal environments (Yao et al., 2018). Accordingly, the concentrations of Ca and Sr in this section are significantly higher than the silt-clay section, particularly in the top 10 cm of the core. The findings suggest that the surface material of core ROC-4 carries a strong marine signal, likely originating from littoral sources.

4.3 Pollen data

A total of 26 pollen and spore taxa were identified from core ROC-4, but only palynomorphs occurring at > 2% in any interval were shown individually in Figure 2. All minor pollen taxa (< 2%) were grouped together as "other upland taxa" and "other swamp taxa" in Figure 2. The pollen assemblage in Zone A (525-390 cm; ~5190 - 4240 cal yr BP) is dominated by TCT (Taxodiaceae, Cupressaceae, and Taxaceae), Amaranthaceae, and Poaceae. In particular, the pollen assemblages in most intervals contain 10-20% of TCT, a common swamp taxon, reaching their highest percentages in the core. The percentages of Amaranthaceae (up to 20%), Poaceae (< 20%), *Pinus* (up to 30%), and *Quercus* (up to 20%) are relatively high in most intervals in Zone A. Unlike TCT, these taxa are prolific pollinators that produce enormous amount of pollens (Traverse, 2007). Therefore, based on CONISS (Grimm, 1987) and the relative abundance of TCT, Zone A demonstrates typical palynological features of a swamp environment in Louisiana (Ryu et al., 2018). In addition, the concentrations of charcoal fragments and total pollen sum are at 20000-60000 and 5000-17000 counts/cm^3, respectively (Fig. 2).

Zone B (390-320 cm; ~4240 to 3440 cal yr BP) is dominated by forest taxa. The percentages of *Pinus* and *Quercus* are up to 60% and 25% in this zone, both reaching their highest percentages in the core. On the contrary, the percentages of other major taxa that are common in the Zone A (TCT, Amaranthaceae, and Poaceae) all decrease in Zone B. The concentrations of charcoal fragments and total pollen sum are at 30000-40000 and 9000-16000 counts/cm^3, respectively (Fig. 2). Zone B demonstrates palynological features of a maritime forest environment.

The pollen assemblage in Zone C (320 to 160 cm; ~3340 to 1520 cal yr BP) is characterized by an increase in TCT pollen and a decrease in *Pinus* pollen, a change back to swamp environment from maritime forest environment. Notably, a few grains (< 1%) of *Avicennia* (black mangrove) pollen and a small number of foraminifera linings are also found in Zone C. The concentrations of charcoal fragments and total pollen sum are at 20000-50000 and 12000-15000 counts/cm^3, respectively (Fig. 2).

The pollen assemblage in Zone D (160 to 40 cm; ~1520 to 300 cal yr BP) is characterized by a significant increase in marsh taxa and a 10-fold increase in charcoal fragments (up to 1,800,000 counts/cm^3). The percentages of Amaranthaceae (up to 40%) and Poaceae (up to 25%) reach their highest in the core, while pollen percentages of TCT, *Pinus*, and *Quercus* decease. Particularly, *Batis maritima* starts to appear in the pollen assemblage in this zone and increase towards the top. The pollen of *Sagittaria*, a common marsh plant, begin to appear in Zone D. The pollen assemblage in Zone D exhibits typical palynological features of a coastal marsh environment.

Zone E (40 to 0 cm; 300 cal yr BP to present) is characterized by the dominance of *Batis maritima* (saltwort) pollen. This taxon accounts for 30% of the total pollen sum at the bottom of the zone, increasing toward the top of the core where it reaches over 80% of the total pollen sum. Accordingly, the pollen concentration also significantly increases in Zone E because *Batis maritima* is a very prolific pollen producer (Traverse, 2007). Meanwhile, all the other pollen taxa decrease in most intervals. Noticeably, significant increase in foraminifera linings also occurs in this zone. These palynological features resemble a typical beach and saltmarsh environment in southwest Louisiana (Yao et al., 2018).

4.4 Numerical Analysis of pollen data

Percentage data of 12 major pollen taxa (defined as those occurring at and > 5% in most intervals) were used in a PCA. On the PCA biplot showing the distribution of pollen assemblages and 12 major pollen taxa (Fig. 3), the first two principal components (PC) account for 29.83% and 21.41% of the variance, respectively (Table S1-S4). Along PC1 axis, *Batis maritima*, a succulent plant thriving in saline environment, have the highest positive loading, whereas bottomland hardwood forest species (*Pinus*, *Liquidambar*, and *Quercus*) have the highest negative loadings. It is likely that PC1 represents a salinity gradient whereby salinity increases from negative toward the positive end of the axis. On PC2, trees and succulent plants (*Pinus*, *Liquidambar*, and *Batis maritima*) have the highest positive loadings. All three taxa, especially *Batis maritima*, adapt to dry or upland environment (Traverse, 2007). At the other end of the axis, wetland and aquatic plants (Poaceae, Cyperaceae, Asteraceae, and *Sagittaria*) have the highest negative loadings. All these taxa, especially *Sagittaria*, an emergent macrophyte, can adapt to water-logged or wetland environment (Traverse, 2007). Thus, it is reasonable to infer that PC2 denotes a hydrological gradient reflecting the moisture content. Accordingly, the PCA biplot is divided into 4 quadrants representing 4 sub-environments, in a clockwise direction, which are Beach (dry and saline), Marsh (wet and saline), Swamp (wet and fresh), and Maritime forest (dry and fresh) environment.

Figure 3A shows the distribution of all pollen assemblages on the PCA biplot, and Figure 3B shows the total pollen sum of each ecological group following the inferred pollen zonation discussed in Figure 2. From the bottom to the top of the core, numerical analysis of pollen data shows that all samples in Zone A fall into the Swamp quadrant (bottom left); all samples in Zone B are located in the Maritime forest quadrant (top left); most samples in Zone C fall back into the Swamp quadrant (bottom left); all samples in Zone D belong to the Marsh quadrant (bottom right); and all samples in Zone E fit exclusively in the Beach quadrant (top right). Hence, the PCA of pollen assemblages is consistent with the inferred pollen zones delineated by CONISS.

5. Discussion

5.1 Holocene coastal morphodynamics and ecosystem development in southwestern Louisiana

Overall, the sedimentary and geochemical datasets show consistent stratigraphic features throughout the core (Fig. 2), suggesting that most intervals within a zone in the sediment profile originated from the same sediment source. Figure 4 illustrates the inferred shoreline and paleoecological history at Rockefeller Wildlife Refuge since the mid-Holocene based on numerical and empirical analyses of pollen data, in relation to the established phases of Mississippi River Delta development (Fig. 4). Between 5190 and 4240 cal yr BP, numerical analysis shows that the pollen assemblage in Zone A is consistent with the pollen signature of a freshwater swamp in Louisiana (Figs. 2 & 3) (Ryu et al., 2018). Such areas are dominated by baldcypress (*Taxodium distichum*), a deciduous conifer most commonly found in freshwater swamps (Lopez, 2003). These ecosystems are typically located in areas 50-100 km inland from the Gulf shorelines (Glick et al., 2013). Thus, our record suggests that the relative sea-level (RSL) was much lower than the present level from 5190 to 4240 cal yr BP, and the shoreline at RWR was likely many kilometers seaward relative to today.

In the meantime, to the east of RWR, the Sale-Cypremont complex (4600-3500 BP), situated at the westernmost position and the closest to our study area among the 6 complexes, was forming during the end of the freshwater swamp stage (Fig. 4). Concurrently, pollen data indicate that the baldcypress swamp in our study area was replaced by *Pinus*, *Quercus*, and *Liquidambar* (Fig. 2), a transition from a longer-hydroperiod freshwater swamp to a dryer maritime forest during 4240-3440 cal yr BP (Fig. 3). Along a typical vegetation zonation pattern across coastal zones in North America, maritime forests occupy areas further inland from freshwater swamps (Traverse, 2007). Hence, shorelines at the RWR was further seaward during the maritime forest stage relative to the freshwater swamp stage (Fig. 4). Such vegetation transition at RWR was consistent with the cyclic delta-building process of the Mississippi River that when the delta lobe switched to a western position, significantly higher suspended sediment load from the Mississippi River would have been transported to the west by the longshore currents - replenishing the coastal zones and resulting in shoreline progradation in southwestern Louisiana (McBride et al., 2007; Owen, 2008; Rosen and Xu, 2011). In particular, the development of maritime forest, which was made possible by shoreline progradation in our study area during 4240-3440 cal yr BP, was synchronous with the timeline of the Sale-Cypremont complex (4600-3500 BP). Thus, all the evidence so far suggests that the Mississippi River Delta Complex is closely associated with the coastal morphodynamics and ecosystem development in southwestern Louisiana.

Nevertheless, when the Mississippi River changed its course to the east during the next two delta cycles (Teche and St. Bernard), the Holocene geomorphological history of the southwestern Louisiana coastlines reached a turning point at 3440 cal yr BP when the shoreline dynamics changed from progradational to retrogradational (Fig. 4). This transition is clearly recorded by the proxy record (Figs. 2 & 3). Baldcypress pollen started to rise again in Zone C (3440-1520 cal yr BP), while the maritime forest taxa started to decrease. Although marine influence was still negligible during this period, this vegetation transition was in contrast to Zones A & B. The transition from maritime forest back to baldcypress swamp suggests a gradual rising of the water table, hence, clear evidence of shoreline retreat in our study area.

The pollen evidence suggests that shoreline retreat continued throughout Zone D (1520-300 cal yr BP). With the delta lobe remaining at an eastern position during the Lafourche (1000-300 BP) and Plaquemine-Balize (750 BP to present) phases (Fig. 4), the freshwater swamp taxa at RWR were progressively replaced by marsh taxa (Fig. 3). Furthermore, foraminifera linings, an indicator of marine environment, started to appear with greater regularity during this period. Sand fraction also started to increase in Zone D, indicating a more dynamic environment with higher wave energy (Xu et al., 2016, 2011). In addition, the halophyte *Batis maritima* started to appear while baldcypress declined (Fig. 2). Historically, cypress swamp degradation in Louisiana is attributed to erosion and saltwater intrusion (Roberts, 1997; Glick et al., 2013; Liu et al., 2015;Ryu et al., 2018). These evidences suggest that our study area was turning into a coastal marsh environment with more marine influence. Today, similar coastal marsh occurs as an ecotone between freshwater swamp and beach ridge in RWR (Selman et al., 2011; Yao et al., 2018). Using it as a modern analog, it could be inferred that between 1500 and 300 cal yr BP, freshwater environment at RWR was transforming into brackish marsh environment as marine retrogradation continued.

Finally, since ~400 yr BP, while the main distributary basin of the Mississippi River - Plaquemine-Balize complex remained active, a second distributary basin - the Atchafalaya-Wax Lake complex formed in southwestern Louisiana (Fig. 4). Based on 31 years (1980–2010) of total suspended sediment inflow/outflow data, the Atchafalaya River was delivering ~33 megaton (10^6 tons) of total suspended sediments (TSS) to the Gulf every year (Rosen and Xu, 2015), resulting in a net land gain of 59 km^2 (1989-2010) in the basin (Rosen and Xu, 2013). However, situated at ~100 km to the west of Atchafalaya River mouth, the shoreline at RWR was not replenished by such enormous sediment input (Fig. 5). The pollen data show that *Batis maritima* kept increasing from 300 cal yr BP and became the dominant taxon in Zone E. Meanwhile, other marine indicators including sand fraction (Xu et al., 2016), % carbonate (Yao and Liu, 2017), concentration of Ca and Sr (Yao and Liu, 2018; Yao et al., 2019), and foraminifera linings (Yao et al., 2018) all increased significantly in Zone E. This multi-proxy signature highly resembles the shelly beach environment occurring at the interface between coastal marshes and the Gulf at RWR today (Selman et al., 2011; Yao et al., 2018). The pollen concentration also increased significantly at ~300 cal yr BP, coincident with the increase in *Batis maritima*, a prolific pollen producer. Therefore, the modern beach environment replaced the marsh environment at RWR since 300 cal yr BP due to shoreline retrogression, even though two new sub-deltas (the Atchafalaya and the Wax Lake deltas) formed to the east of our study area (Fig. 4). Overall, when the Mississippi River Delta was at its westerly position as during the Sale-Cypremont phase 4600-3500 years ago, the shoreline at RWR was prograding and our coring site was situated farther inland from the coast. Conversely, when the Mississippi River Delta lobe switched to more easterly positions during the subsequent Teche, St. Bernard, Lafourche, and Plaquemine-Balize phases, shoreline retrogression at RWR started at ~3340 cal yr BP and continued to the present day. Thus, shoreline fluctuations at RWR were tied to the Mississippi River Delta Switch (Fig. 4). Table S5 in the supplementary content synthesize the multi-proxy dataset and further elaborates the correspondences among different systems.

5.2 Evidence of possible paleohurricane events

Several sediment intervals in the core show signs of possible disturbance events. Higher sand and silt fractions were found at 320, 280, 100, and 50 cm, and elevated Ca and Sr concentrations occur at 280, 200, 140, and 20-0 cm. Higher contents of sand (Williams, 2009), Ca, and Sr have been described as indicators of prehistorical hurricane events (Woodruff et al., 2009; Yao et al., 2018; McCloskey et al., 2018). While any one of these lines of evidences may not be conclusive indicators of paleohurricane events *per se*, it is notable that at least two of the stratigraphic levels, at 280 cm and 200 cm, are marked by elevated concentrations of Ca and Sr, and/or higher sand and silt fractions. It is also interesting that these levels containing these characteristics occur during the time interval between ~3000 and 900 years BP, generally corresponding to the “hyperactive period” (~3800-1000 al yr BP) in paleohurricane activity documented in the Gulf of Mexico (Liu and Fearn, 2000) and the Caribbean basin (Giry et al. 2012; Aragón-Moreno et al. 2018). It is therefore possible that increased hurricane activities in the Gulf of Mexico directly or indirectly affected southwestern Louisiana during the hyperactive period.

The biggest of these possible hurricane events, marked by prominent peaks in both Ca and Sr, occurred at 200 cm (~2000 cal yr BP) near the top of Zone C, at a time when the coring site was transitioning from a swamp to a marsh as the shoreline was retreating, making the site more vulnerable to storm surge from extreme hurricanes than before. Another possible event layer, occurring at 100 cm (~900 cal yr BP) in the upper part of Zone D, is marked by a greater fraction of sand. While this could be deposited by storm surge or overwash processes during a paleohurricane event, this explanation cannot be firmly established as it is not supported by any corroborating evidence from the marine incursion proxies such as Ca and Sr. Alternatively, other disturbance mechanisms, such as fluvial flooding from extreme precipitation events, could be responsible for the deposition of sand layers in coastal wetland sediments (Wang et al., 2019). However, no large rivers are present near our study site today.

The uppermost 20 cm of the sediment core from Louisiana’s Chenier Plain is marked by prominent peaks in carbonates, Ca and Sr concentrations, and the abundance of foraminifera tests and shells. In a geochemical study of the nearby Calcasieu River estuary, He and Xu (2016) found a strong increasing trend of these two elements from upstream to the river mouth. These findings strongly suggest marine incursion and/or overwash events caused by hurricane activity. Multi-proxy data from three sediment monoliths collected within 50 m from the coring site contained two storm deposits attributed to two recent hurricanes—Hurricane Ike (2008) and Hurricane Rita (2005)—in the top 20 cm (Yao et al., 2018). These two storm deposits are similarly represented in the upper 20 cm of core ROC-4. An analysis of remote sensing images from 1998 to 2017 showed that the shoreline at RWR retreated by 276 m over this 20-year period, at a rate of 14.5 m/year—the highest rate of coastal recession in the entire Gulf of Mexico (Yao et al., 2018; Dietz et al., 2018) (Fig. 5). During the last 300 years (Zone E) rapid shoreline retreat has rendered the coring site into a backbarrier setting behind a shelly beach and berm, thereby becoming increasingly subject to the impacts of storm surge and overwash processes. Thus, the impacts of these two recent hurricanes are prominently recorded in the stratigraphy of core ROC-4.

5.3 Implications for coastal morphodynamics and sustainability in southwestern Louisiana

The multi-proxy record in this study has demonstrated that coastal morphodynamics in southwestern Louisiana was closely tied to the position of the Mississippi River Delta complexes (Fig. 4). During the mid-Holocene when the main Mississippi River Delta was situated in the west (i.e., the Sale-Cypremont complex), sedimentation rate at RWR was 1.44 mm/yr—roughly equal to the rate of RSL rise (1.5 mm/ yr) at that time (Törnqvist et al., 2004)—the shoreline at RWR was prograding due likely to sufficient sediment supplies by the Mississippi-Atchafalaya River system. Subsequently, when the delta switched to more easterly positions (Teche, St. Bernard, Lafourche, and Plaquemine-Balize complexes) after 3500 yr BP, sedimentation rate at RWR decreased to 0.88 mm/yr, a decrease of almost 40% and slower than the rate of regional sea-level rise (~1 mm/yr) (Donoghue, 2011), causing the shoreline at RWR to retreat rapidly. During the past 300 years when the Atchafalaya-Wax Lake complex developed in areas closer to southwest

Louisiana, sedimentation rate at RWR increased to 1.19 mm/yr. However, the modern rate of RSL rise in Louisiana also increased to almost twice as high (2 mm/yr) (Penland and Ramsey, 1990; Donoghue, 2011), thereby resulting in accelerated coastal retrogression. The shoreline at RWR was retreating at an alarming rate of 14.5 m/yr since the 1990s (Fig. 5), and this rate was even higher during years with hurricane strikes (Yao et al., 2018). These numbers exhibit a strong relationship between shoreline fluctuations and the rate of sedimentation versus the rate of RSL rise. When the sedimentation rate exceeds the rate of RSL, the shoreline at RWR is sustained. Conversely, when the sedimentation rate falls lower than the rate of RSL rise, the shoreline at RWR retreats, resulting in significant land loss in southwestern Louisiana. The driving force behind the variations in sedimentation rate at RWR is the position of the Mississippi River Delta, which is the main source of sediment supply for the coastal plain of southwestern Louisiana.

At present, the Atchafalaya River is the main source of sediment supply for the southwestern Louisiana coastlines (Xu, 2010; Rosen and Xu, 2011). The Atchafalaya-Wax Lake complex annually delivers ~30% of Mississippi River's water and 33 megatons of total suspended sediments (TSS) into the Gulf of Mexico (Rosen and Xu, 2015). However, this amount of annual sediment supply is insufficient to counter the rate of RSL rise and to replenish the coastal wetlands at RWR. This condition is reflected in the delicate location where RWR is situated at today with regard to Louisiana's coastal morphodynamics, whereby the shorelines to the east are rapidly prograding due to sufficient sediment supply from the Atchafalaya River (Xu, 2010; Rosen and Xu, 2013) but the Chenier Plain to the west is rapidly eroding as the distance from the Atchafalaya River mouth increases (Roberts, 1997; McBride et al., 2007; Owen, 2008; Rosen and Xu, 2011). Although the TSS input from the Plaquemine-Balize delta complex, the main delta of the modern Mississippi River, is much higher, this sediment source is over 300 km to the east of RWR – too far and too negligible to replenish the wetlands on the southwestern Louisiana coastlines (Xu, 2010; Wang and Xu, 2018). The four minor rivers in southwestern Louisiana - Sabine, Calcasieu, Mermentau, and Vermilion Rivers (Fig. 1), totally carried 6.86 x 10^6 tons of sediments over a 20-year period from 1990-2010, but most of this sediment was unable to reach the coastline, and the portion that did reach the coastline was transported to Texas by the long-shore currents (Rosen and Xu, 2011). Therefore, increasing the sediment supply from the Atchafalaya River to the east is the only viable option to combat shoreline retreat and coastal land loss in RWR and southwestern Louisiana.

One possible solution for replenishing the coastal wetlands at RWR will be to divert more sediments from the main Mississippi River—now carrying about 75% of the annual discharge—to the Atchafalaya River via the Old River Control Structure near Red River Landing, Louisiana (Rosen and Xu, 2013; 2015). However, this will further reduce the sediment supply to the already sinking southeastern Louisiana coasts, especially around the bird-foot delta (Wang and Xu, 2018). In fact, the State of Louisiana has proposed in its 2017 Coastal Master Plan (CPRA, 2017) that sediment diversions from the lower Atchafalaya to the east Terrebonne Parish be implemented, which could further reduce riverine sediment supply to the Chenier Plain. All the four nearby rivers flowing through Louisiana's Chenier Plain deliver only a marginal quantity of sediment (in total: 3.43 x 10^5 tons per year) to the chenier coast, and the sediment load has been declining (Rosen and Xu, 2011). Therefore, the restoration of coastal Louisiana is facing a dilemma of either saving one side of the coast or losing both sides.

6. Conclusions

This study utilizes a multi-proxy approach to reconstruct the sedimentary and ecological history of the Chenier Plain in southwestern Louisiana, one of the world's largest chenier plains, which is located west of the Mississippi-Atchafalaya River system. The findings from this study suggest a strong influence of the river on the development of the Chenier Plain and its ecosystems in the past 5,200 years. Since the mid-Holocene, the shoreline of the Chenier Plain fluctuated between progradation and retrogradation, and this fluctuation was closely tied to the Mississippi River Delta Switch. The pollen record shows that coastal ecosystems at the eastern end of Louisiana's Chenier Plain changed from swamp to maritime forest during 5200-3440 cal yr BP, and from swamp to marsh and then to beach/dune community after 3440 cal yr BP. Shoreline retrogradation at the study site began around ~3440 cal yr BP and persisted to the present day. In particular, the shoreline at the Rockefeller Wildlife Refuge was retreating at an alarming rate of 14.5 m/yr since the 1990s. The shoreline fluctuation and the rate of sedimentation are also associated with the rate of relative sea level rise. When the sedimentation rate falls below the relative sea level rise rate, the shoreline of the Chenier Plain retrogrades, resulting in significant land loss in southwestern Louisiana. Based on these findings, we conclude that Louisiana's Chenier Plain will continue to retreat because of the continuous sea level rise and reduction of riverine sediment supply.

Acknowledgements

This research was supported by grants from the U.S. National Science Foundation (Grants #1759715, 1212112), NOAA/Louisiana Sea Grant, Louisiana Coastal Protection and Restoration Authority (CPRA Coastal Science Scholarship funds), and the Ministry of Science and Technology of the People's Republic of China (Grant #2017YFE0107400). During the preparation of the manuscript, Y. Jun Xu received funding support from a US Department of Agriculture Hatch Fund project (project number: LAB94230). The statements, findings, and conclusions are those of the authors and do not necessarily reflect the views of the funding agencies. We thank Terrence McCloskey, Thomas Bianchette, and Joanna Plattsmier for their assistance in fieldwork. Special thanks go to Phillip "Scooter" Trosclair and other staff members from the Rockefeller Wildlife Refuge for field and logistical support during this study.

Data Availability

All of the datasets produced in this article will be stored at the Neotoma Paleoecology Database (https://www.neotomadb.org) upon publication and accessible to the public for free.

Figure Captions

Figure 1. Location of the sediment core ROC-4 (red star) at the eastern end of the Chenier Plain in southwestern Louisiana, USA. Sediment supply in the area is strongly influenced by the Mississippi River, which changed its course several times in the past 5,000 years (in chronological order based on Roberts, 1997; Day et al., 2007; and McBride et al., 2007).

Figure 2. The age-depth model, litholog, grain-size, LOI, XRF, and pollen results of core ROC-4 from southwestern Louisiana.

Figure 3. (A) PCA biplot showing the distribution of 12 main pollen taxa and pollen assemblages collected from core ROC-4, plotted along components 1 and 2. (B) Vegetation sub-environments on the chenier plain based on CONISS and PCA biplot.

Figure 4. (Left) Conceptual diagram illustrating the Holocene coastal morphodynamics and ecosystem development on Louisiana's Chenier Plain at the Rockefeller Wildlife Refuge; (Right) corresponding developmental phases of the Mississippi River Delta Switch.

Figure 5. Remote sensing images showing rapid shoreline retrogradation on Louisiana's Chenier Plain at the Rockefeller Wildlife Refuge from 1998 to 2017. The red lines perpendicular to the shoreline show the distance between the core ROC-4 location and the seaward edge of the beach (the white area on satellite image) on every satellite image. These lines were used as references to measure the site-to-sea distance for when the satellite image was taken. The figure is a modified version from that in Yao et al. (2018).

Table Caption

Table 1. Radiocarbon dating results for core ROC-4 from southwestern Louisiana.

References

Aragón-Moreno, A.A., Islebe, G.A., Roy, P.D., Torrescano-Valle, N., Mueller, A.D., 2018. Climate forcings on vegetation of the southeastern Yucatán Peninsula (Mexico) during the middle to late Holocene. Palaeogeogr. Palaeoclimatol. Palaeoecol. 495, 214–226.

Blum, M.D., Roberts, H.H., 2009. Drowning of the Mississippi Delta due to insufficient sediment supply and global sea-level rise. Nat. Geosci. 2, 488–491.

Bush, N., Bush, E., Sokolova, Y., Bush, N., Blanchard, P., 2018. Utilizing the physiological adaptation mechanisms of coastal plants for vegetative restoration of barrier islands. Ocean Coast. Manag. 161, 222–227.

Chmura, G.L., Stone, P.A., Ross, M.S., 2006. Non-pollen microfossils in Everglades sediments. Rev. Palaeobot. Palynol. 141, 103–119.

Coleman, J.M., 1988. Dynamic changes and processes in the Mississippi River delta. GSA Bulletin 100, 999–1015.

Coleman, J.M., Roberts, H.H., Gregory W. Stone, 1998. Mississippi River Delta: An Overview. J. Coast. Res. 14, 699–716.

Couvillion, B.R., Barras, J.A., Steyer, G.D., Sleavin, W., Fischer, M., Beck, H., Trahan, N., Griffin, B., Heckman, D., 2011. Land area change in coastal Louisiana from 1932 to 2010.

Couvillion, B.R., Beck, H., 2013. Marsh Collapse Thresholds for Coastal Louisiana Estimated Using Elevation and Vegetation Index Data. J. Coast. Res. 63, 58–67.

Couvillion, B.R., Beck, H., Schoolmaster, D. and Fischer, M., 2017. Land area change in coastal Louisiana (1932 to 2016) (No. 3381). US Geological Survey.

CPRA, 2007. Coastal Protection and Restoration Authority, 2017 Coastal Master Plan http://coastal.la.gov/our-plan/2017-coastal-master-plan/ (accessed February 2020).

CPRA, 2020. Coastal Protection and Restoration Authority [WWW Document]. Louisiana Coastal

Protection and Restoration Authority. URL http://coastal.la.gov/ (accessed 1.20).
Day, J.W., Jr, Boesch, D.F., Clairain, E.J., Kemp, G.P., Laska, S.B., Mitsch, W.J., Orth, K., Mashriqui, H., Reed, D.J., Shabman, L., Simenstad, C.A., Streever, B.J., Twilley, R.R., Watson, C.C., Wells, J.T., Whigham, D.F., 2007. Restoration of the Mississippi Delta: lessons from Hurricanes Katrina and Rita. Science 315, 1679–1684.
Dean, W.E., 1974. Determination of carbonate and organic matter in calcareous sediments and sedimentary rocks by loss on ignition; comparison with other methods. J. Sediment. Res. 44, 242–248.
Delcourt, P.A., Delcourt, H.R., 1996. Quaternary paleoecology of the Lower Mississippi Valley. Eng. Geol. 45, 219–242.
Delcourt, P.A., Delcourt, H.R., Brister, R.C., Lackey, L.E., 1980. Quaternary Vegetation History of the Mississippi Embayment 1 , 2. Quat. Res. 13, 111–132.
Dietz, M., Liu, K.-B., Bianchette, T., 2018. Hurricanes as a Major Driver of Coastal Erosion in the Mississippi River Delta: A Multi-Decadal Analysis of Shoreline Retreat Rates at Bay Champagne, Louisiana (USA). Water 10, 1480.
Donnelly, J.P., Webb, T., III, Murnane, R., Liu, K.-B., 2004. Backbarrier sedimentary records of intense hurricane landfalls in the northeastern United States. Hurricanes and Typhoons: Past, Present, and Future 55, 58–95.
Donoghue, J.F., 2011. Sea level history of the northern Gulf of Mexico coast and sea level rise scenarios for the near future. Clim. Change 107, 17.
Elsner, J.B., Jagger, T.H., Liu, K.-B., 2008. Comparison of Hurricane Return Levels Using Historical and Geological Records. J. Appl. Meteorol. Climatol. 47, 368–374.
Frazier, D.E., 1967. Recent deltaic deposits of the Mississippi River: their development and

chronology. Gulf Coast Association of Geological Societies, Transactions 17, 287–316.

Givens, C.R., Givens, F.M., 1987. Age and Significance of Fossil White Spruce (Picea glauca), Tunica Hills, Louisiana-Mississippi. Quat. Res. 27, 283–296.

Giry, C., Felis, T., Kölling, M., Scholz, D., Wei, W., Lohmann, G. and Scheffers, S., 2012. Mid- to late Holocene changes in tropical Atlantic temperature seasonality and interannual to multidecadal variability documented in southern Caribbean corals. Earth and Planetary Science Letters, 331, pp.187-200.

Glick, P., Clough, J., Polaczyk, A., Couvillion, B., Nunley, B., 2013. Potential Effects of Sea-Level Rise on Coastal Wetlands in Southeastern Louisiana. J. Coast. Res. 63, 211–233.

Grimm EC, 1987. CONISS: a Fortran 77 program for stratigraphically constrained cluster analysis by the method of incremental sum of squares. Computers & Geosciences 13(1): 13-35, DOI 10.1016/0098-3004(87)90022-7.

He, S. and Y.J. Xu. 2016. Spatiotemporal Distributions of Sr and Ba along an Estuarine River with a Large Salinity Gradient to the Gulf of Mexico. Water doi: 10.3390/w8080323.

Huntley, B. and Webb III, T. eds., 2012. Vegetation history (Vol. 7). Springer Science & Business Media.

Jones, M.C., Wingard, G.L., Stackhouse, B., Keller, K., Willard, D., Marot, M., Landacre, B., E Bernhardt, C., 2019. Rapid inundation of southern Florida coastline despite low relative sea-level rise rates during the late-Holocene. Nat. Commun. 10, 3231.

Kemp, G.P., Day, J.W., Yáñez-Arancibia, A., Peyronnin, N.S., 2016. Can Continental Shelf River Plumes in the Northern and Southern Gulf of Mexico Promote Ecological Resilience in a Time of Climate Change? Water 8, 83.

Kiage, L.M., 2020. A 1200-year history of environmental changes in Bay Jimmy area, coastal

Louisiana, USA. Holocene 30, 201–209.

Kiage, L.M., Liu, K.-B., 2009. Palynological evidence of climate change and land degradation in the Lake Baringo area, Kenya, East Africa, since AD 1650. Palaeogeogr. Palaeoclimatol. Palaeoecol. 279, 60–72.

King, J.E., Allen, W.H., 1977. A Holocene Vegetation Record from the Mississippi River Valley, Southeastern Missouri. Quat. Res. 8, 307–323.

Kolb, C.R., Van Lopik, J.R., 1958. Geology of the Mississippi River deltaic plain, southeastern Louisiana: US Army Corps of Engineers, Waterways Experiment Station. Technical Report 2.

Kulp, M., Penland, S., Williams, S.J., Jenkins, C., Flocks, J., Kindinger, J., 2005. Geologic Framework, Evolution, and Sediment Resources for Restoration of the Louisiana Coastal Zone. J. Coast. Res. 56–71.

Lam, N.S.-N., Xu, Y.J., Liu, K.-B., Dismukes, D.E., Reams, M., Pace, R.K., Qiang, Y., Narra, S., Li, K., Bianchette, T.A., Cai, H., Zou, L., Mihunov, V., 2018a. Understanding the Mississippi River Delta as a Coupled Natural-Human System: Research Methods, Challenges, and Prospects. Water 10, 1054.

Lam, N.S.-N., Cheng W., Zou L., Cai H., 2018b. Effects of landscape fragmentation on land loss. Remote Sensing of Environment 209:253-262.

Liu, K.-B. and Fearn, M.L., 2000. "Reconstruction of prehistoric landfall frequencies of catastrophic hurricanes in northwestern Florida from lake sediment records", Quaternary Research 54: 238-245.

Liu, K.-B., 2004. Paleotempestology: Principles, methods and examples from Gulf coast lake sediments, in: Murnane, R.J., Kam-biu, L. (Eds.), Hurricanes and Typhoons: Past, Present and Future. New York: Columbia University Press.

Liu, K.-B., Lam, N.S.-N., 1985. Paleovegetational Reconstruction Based on Modern and Fossil Pollen Data: An Application of Discriminant Analysis. Ann. Assoc. Am. Geogr. 75, 115–130.

Liu, K.-B., Li, C., Bianchette, T.A., McCloskey, T.A., Yao, Q., Weeks, E., 2011. Storm deposition in a coastal backbarrier lake in Louisiana caused by Hurricanes Gustav and Ike. J. Coast. Res. 1866–1870.

Liu, K.-B., McCloskey, T.A., Ortego, S., Maiti, K., 2014. Sedimentary signature of Hurricane Isaac in a Taxodium swamp on the western margin of Lake Pontchartrain, Louisiana, USA. Proceedings of the International Association of Hydrological Sciences 367, 421–428.

Lopez, J.A., 2003. Chronology and analysis of environmental impacts within the Pontchartrain basin of the Mississippi Delta Plain: 1718-2002. University of New Orleans.

McAndrews, J.H., Berti, A.A., Norris, G., 1973. Key to the quaternary pollen and spores of the Great Lakes region. Royal Ontario Museum.

McBride, R.A., Taylor, M.J., Byrnes, M.R., 2007. Coastal morphodynamics and Chenier-Plain evolution in southwestern Louisiana, USA: A geomorphic model. Geomorphology 88, 367–422.

McFarlan, E., Jr, 1961. Radiocarbon dating of late Quaternary deposits, south Louisiana. Geol. Soc. Am. Bull. 72, 129–158.

McIntire, W.G., 1954. Correlation of prehistoric settlements and delta development. Louisiana State University.

Michot, T.C., Day, R.H., Wells, C.J., 2010. Increase in black mangrove abundance in coastal Louisiana. Louisiana Natural Resources News.

Owen, D.E., 2008. Geology of the Chenier Plain of Cameron Parish, southwestern Louisiana. Geological Society of America Field Guide 14, 27–38.

Osland, M.J., et al., 2013. Winter climate change and coastal wetland foundation species: salt marshes vs. mangrove forests in the southeastern United States. Global Change Biology 19(5): 1482-1494.

Penland, S., Ramsey, K.E., 1990. Relative Sea-Level Rise in Louisiana and the Gulf of Mexico: 1908-1988. J. Coast. Res. 6, 323–342.

Reed, D.J., Wilson, L., 2004. Coast 2050: A New Approach to Restoration of Louisiana Coastal Wetlands. Phys. Geogr. 25, 4–21.

Roberts, H.H., 1997. Dynamic Changes of the Holocene Mississippi River Delta Plain: The Delta Cycle. J. Coast. Res. 13, 605–627.

Rosen, T., Xu, Y.J., 2015. Estimation of sedimentation rates in the distributary basin of the Mississippi River, the Atchafalaya River Basin, USA. Hydrology Research 46, 244–257.

Rosen, T., Xu, Y.J., 2013. Recent decadal growth of the Atchafalaya River Delta complex: Effects of variable riverine sediment input and vegetation succession. Geomorphology 194, 108–120.

Rosen, T., Xu, Y.J., 2011. Riverine sediment inflow to Louisiana Chenier Plain in the Northern Gulf of Mexico. Estuar. Coast. Shelf Sci. 95, 279–288.

Ryu, J., Bianchette, T.A., Liu, K.-B., Yao, Q., Maiti, K.D., 2018. Palynological and Geochemical Records of Environmental Changes in a Taxodium Swamp near Lake Pontchartrain in Southern Louisiana (USA) during the Last 150 Years. J. Coast. Res. 85, 381–385.

Schoolmaster, D.R., Stagg, C.L., Sharp, L.A., McGinnis, T.E., Wood, B., Piazza, S.C., 2018. Vegetation Cover, Tidal Amplitude and Land Area Predict Short-Term Marsh Vulnerability in Coastal Louisiana. Ecosystems 21, 1335–1347.

Selman, W., Salyers, B., Salyers, C., Perry, G., Elsey, R., Hess, T., Zimorski, S., 2011. Rockefeller Wildlife Refuge Management Plan. Grand Chenier: Louisiana Department of Wildlife and

Fisheries.
Shaffer, G.P., Wood, W.B., Hoeppner, S.S., Perkins, T.E., Zoller, J., Kandalepas, D., 2009. Degradation of baldcypress--water tupelo swamp to marsh and open water in southeastern Louisiana, USA: an irreversible trajectory? J. Coast. Res. 2009, 152–165.
Stuiver, M., Reimer, P.J., Reimer, R., 2020. CALIB Radiocarbon Calibration 7.1 [WWW Document]. Calib 7.1. URL http://calib.org/calib/calib.html (accessed 1.31.20).
Schwartz, M. (ed.), 2005. Encyclopedia of Coastal Science. Springer Science & Business Media.
Törnqvist, T.E., González, J.L., Newsom, L.A., Van der Borg, K., De Jong, A.F.M., Kurnik, C.W., 2004. Deciphering Holocene sea-level history on the US Gulf Coast: A high-resolution record from the Mississippi Delta. Geol. Soc. Am. Bull. 116, 1026–1039.
Traverse, A., 2007. Paleopalynology, Topics in Geobiology. Springer.
Urrego, L.E., Bernal, G., Polanía, J., 2009. Comparison of pollen distribution patterns in surface sediments of a Colombian Caribbean mangrove with geomorphology and vegetation. Rev. Palaeobot. Palynol. 156, 358–375.
Van Soelen, E.E., Brooks, G.R., Larson, R.A., Sinninghe Damsté, J.S., Reichart, G.J., 2012. Mid- to late-Holocene coastal environmental changes in southwest Florida, USA. Holocene 22, 929–938.
Wallace, D.J., Woodruff, J.D., Anderson, J.B., Donnelly, J.P., 2014. Palaeohurricane reconstructions from sedimentary archives along the Gulf of Mexico, Caribbean Sea and western North Atlantic Ocean margins. Geological Society, London, Special Publications 388, 481–501.
Wang, B., Xu, Y.J., 2018. Decadal-Scale Riverbed Deformation and Sand Budget of the Last 500 km of the Mississippi River: Insights into Natural and River Engineering Effects on a Large

Alluvial River. Journal of Geophysical Research: Earth Surface 123, 874–890.
Wang, L., Bianchette, T.A. and Liu, K.B., 2019. Diatom evidence of a paleohurricane-induced coastal flooding event in Weeks Bay, Alabama, USA. Journal of Coastal Research, 35(3), 499-508.
Whitehead, D.R., 1972. Developmental and Environmental History of the Dismal Swamp. Ecol. Monogr. 42, 301–315.
Whitehead, D.R., Sheehan, M.C., 1985. Holocene Vegetational Changes in the Tombigbee River Valley, Eastern Mississippi. Am. Midl. Nat. 113, 122–137.
Willard, D.A., Bernhardt, C.E., 2011. Impacts of past climate and sea level change on Everglades wetlands: placing a century of anthropogenic change into a late-Holocene context. Clim. Change 107, 59.
Willard, D.A., Bernhardt, C.E., Weimer, L., Cooper, S.R., Gamez, D., Jensen, J., 2004. Atlas of pollen and spores of the Florida Everglades. Palynology 28, 175–227.
Willard, D.A., Weimer, L.M., Riegel, W.L., 2001. Pollen assemblages as paleoenvironmental proxies in the Florida Everglades. Rev. Palaeobot. Palynol. 113, 213–235.
Williams, K., Pinzon, Z.S., Stumpf, R.P., Raabe, E.A., 1999. Sea-level rise and coastal forests on the Gulf of Mexico. US Geological Survey 1500, 20910.
Williams, J.W., Shuman, B.N., Webb III, T., Bartlein, P.J., Leduc, P.L., 2004. Late-Quaternary vegetation dynamics in North America: scaling from Taxa to Biomes. Ecological Monographs 74(2):309-334
Woodruff, J.D., Donnelly, J.P., and Okusu, A., 2009, Exploring typhoon variability over the mid-to-late Holocene: Evidence of extreme coastal flooding from Kamikoshiki, Japan: Quaternary Science Reviews, v. 28, p. 1774– 1785, doi:10.1016/j.quascirev.2009.02.005.

Xu, K., Harris, C.K., Hetland, R.D., Kaihatu, J.M., 2011. Dispersal of Mississippi and Atchafalaya sediment on the Texas–Louisiana shelf: Model estimates for the year 1993. Cont. Shelf Res. 31, 1558–1575.

Xu, K., Mickey, R.C., Chen, Q., Harris, C.K., Hetland, R.D., Hu, K., Wang, J., 2016. Shelf sediment transport during hurricanes Katrina and Rita. Comput. Geosci. 90, 24–39.

Xu, Y.J., 2010. Long-term sediment transport and delivery of the largest distributary of the Mississippi River, the Atchafalaya, USA. Sediment Dynamics for a Changing Future 337, 282–290.

Xu, Y.J., Lam, N.S.-N., Liu, K.-B., 2018. Assessing Resilience and Sustainability of the Mississippi River Delta as a Coupled Natural-Human System. Water 10, 1317.

Yao, Q., Liu, K.-B., 2018. Changes in Modern Pollen Assemblages and Soil Geochemistry along Coastal Environmental Gradients in the Everglades of South Florida. Frontiers in Ecology and Evolution 5, 178.

Yao, Q., Liu, K.-B., 2017. Dynamics of marsh-mangrove ecotone since the mid-Holocene: A palynological study of mangrove encroachment and sea level rise in the Shark River Estuary, Florida. PLoS One 12, e0173670.

Yao, Q., Liu, K.-B., Platt, W.J., Rivera-Monroy, V.H., 2015. Palynological reconstruction of environmental changes in coastal wetlands of the Florida Everglades since the mid-Holocene. Quat. Res. 83, 449–458.

Yao, Q., Liu, K.-B., Ryu, J., 2018. Multi-proxy Characterization of Hurricanes Rita and Ike Storm Deposits in the Rockefeller Wildlife Refuge, Southwestern Louisiana. Journal of Coastal Research 85, 841–845.

Yao, Q., Liu, K.-B., Williams, H., Joshi, S., Bianchette, T.A., Ryu, J., Dietz, M., 2019. Hurricane

Harvey Storm Sedimentation in the San Bernard National Wildlife Refuge, Texas: Fluvial Versus Storm Surge Deposition. Estuaries Coasts. https://doi.org/10.1007/s12237-019-00639-6

Zhang, Z., Yao, Q., Bianchette, T.A., Liu, K.-B., Wang, G., 2019. A multi-proxy quantitative record of Holocene hydrological regime on the Heixiazi Island (NE China): indications for the evolution of East Asian summer monsoon. Clim. Dyn. 52, 6773–6786.

Figure 1

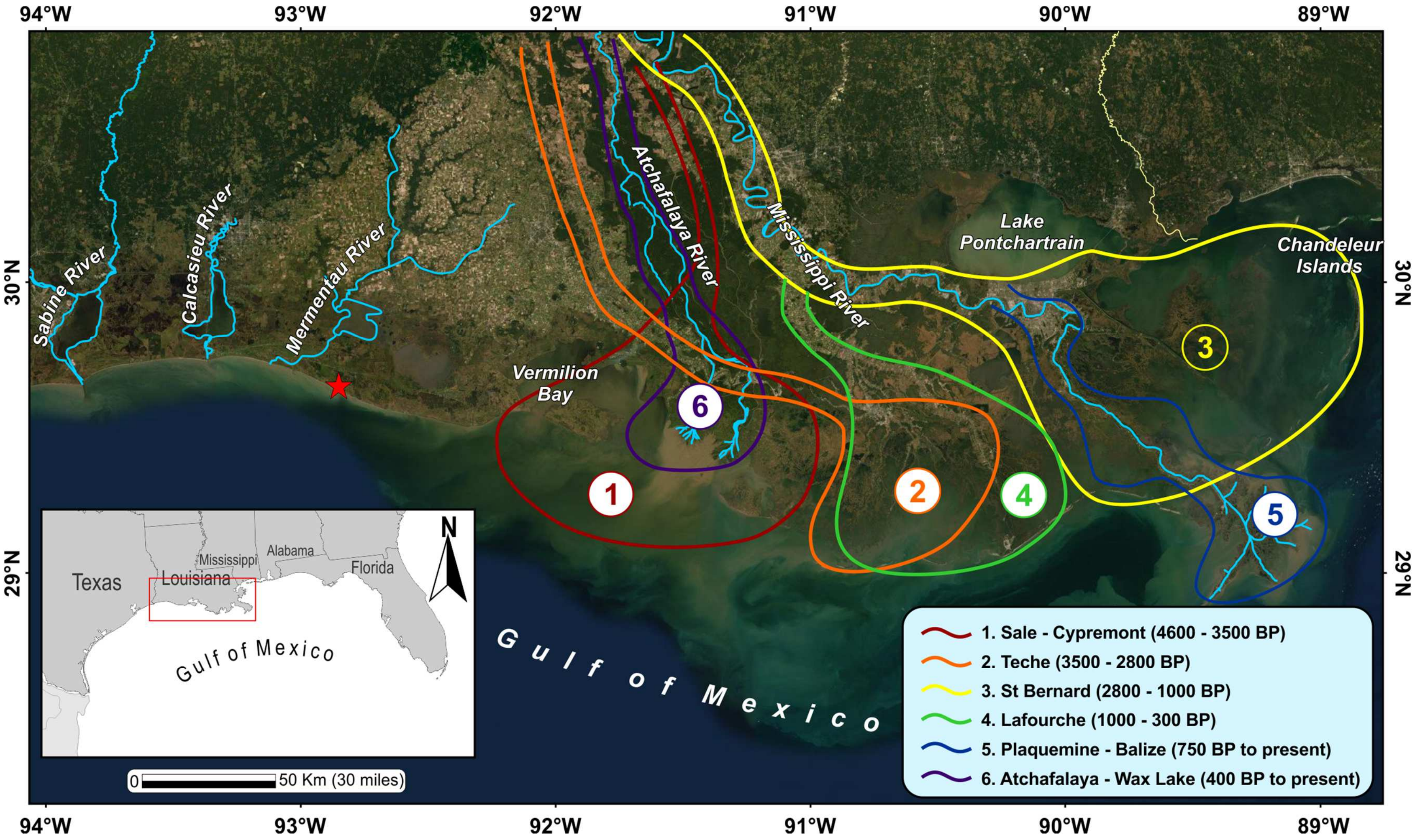
94°W
93°W
92°W
91°W
90°W
89°W
30°N
29°N
Sabine River
Calcasieu River
Mermentau River
Atchafalaya River
Mississippi River
Lake Pontchartrain
Chandeleur Islands
Vermilion Bay
Gulf of Mexico
1
2
3
4
5
6
Texas
Louisiana
Mississippi
Alabama
Florida
N
0
50 Km (30 miles)
1. Sale - Cypremont (4600 - 3500 BP)
2. Teche (3500 - 2800 BP)
3. St Bernard (2800 - 1000 BP)
4. Lafourche (1000 - 300 BP)
5. Plaquemine - Balize (750 BP to present)
6. Atchafalaya - Wax Lake (400 BP to present)

Figure 2

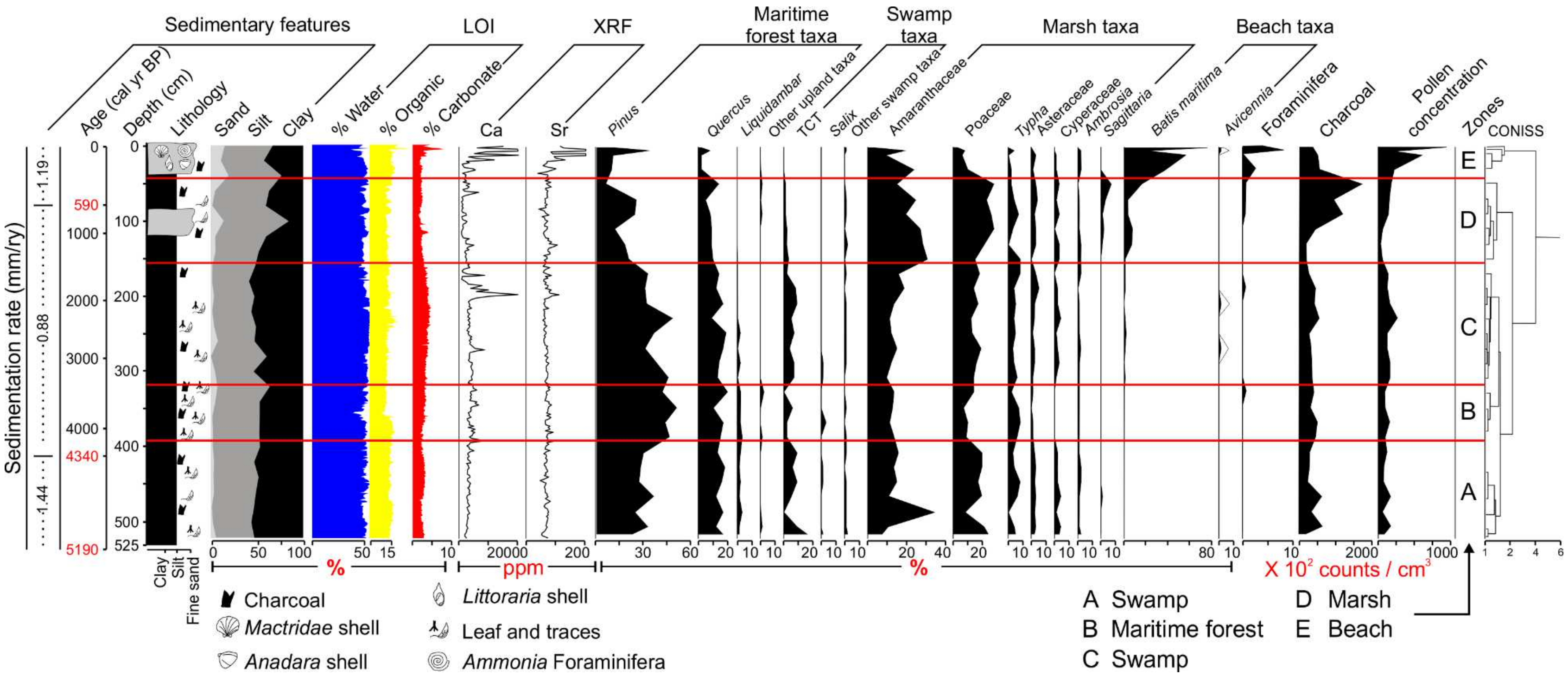

Sedimentary features
LOI
XRF
Maritime forest taxa
Swamp taxa
Marsh taxa
Beach taxa
Age (cal yr BP)
Depth (cm)
Lithology
Sand
Silt
Clay
% Water
% Organic
% Carbonate
Ca
Sr
Pinus
Quercus
Liquidambar
Other upland taxa
TCT
Salix
Other swamp taxa
Amaranthaceae
Poaceae
Typha
Asteraceae
Cyperaceae
Ambrosia
Sagittaria
Batis maritima
Avicennia
Foraminifera
Charcoal
Pollen concentration
Zones
CONISS
Sedimentation rate (mm/ry)
1.19
0.88
1.44
590
1000
2000
3000
4000
4340
5190
Clay
Silt
Fine sand
%
ppm
%
X 10² counts / cm³
Charcoal
Mactridae shell
Anadara shell
Littoraria shell
Leaf and traces
Ammonia Foraminifera
A Swamp
B Maritime forest
C Swamp
D Marsh
E Beach

Figure 3

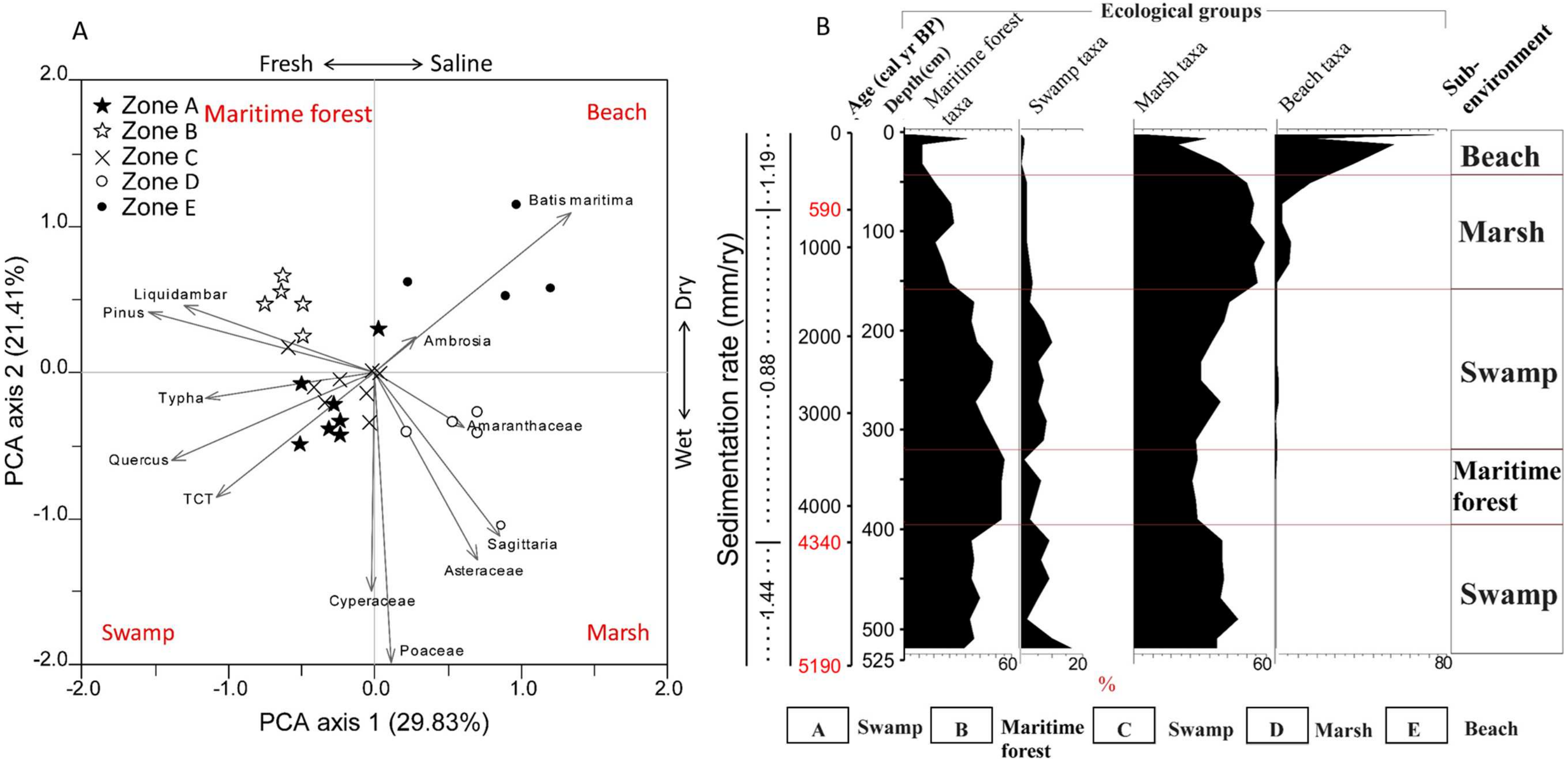

A
Fresh ⟷ Saline
Zone A
Zone B
Zone C
Zone D
Zone E
Maritime forest
Beach
Swamp
Marsh
Batis maritima
Liquidambar
Pinus
Ambrosia
Typha
Amaranthaceae
Quercus
TCT
Sagittaria
Asteraceae
Cyperaceae
Poaceae
Dry
Wet
PCA axis 1 (29.83%)
PCA axis 2 (21.41%)
B
Ecological groups
Age (cal yr BP)
Depth(cm)
Maritime forest taxa
Swamp taxa
Marsh taxa
Beach taxa
Sub-environment
Sedimentation rate (mm/ry)
1.19
0.88
1.44
590
1000
2000
3000
4000
4340
5190
Beach
Marsh
Swamp
Maritime forest
Swamp
%
A Swamp
B Maritime forest
C Swamp
D Marsh
E Beach

747 **Figure 4**

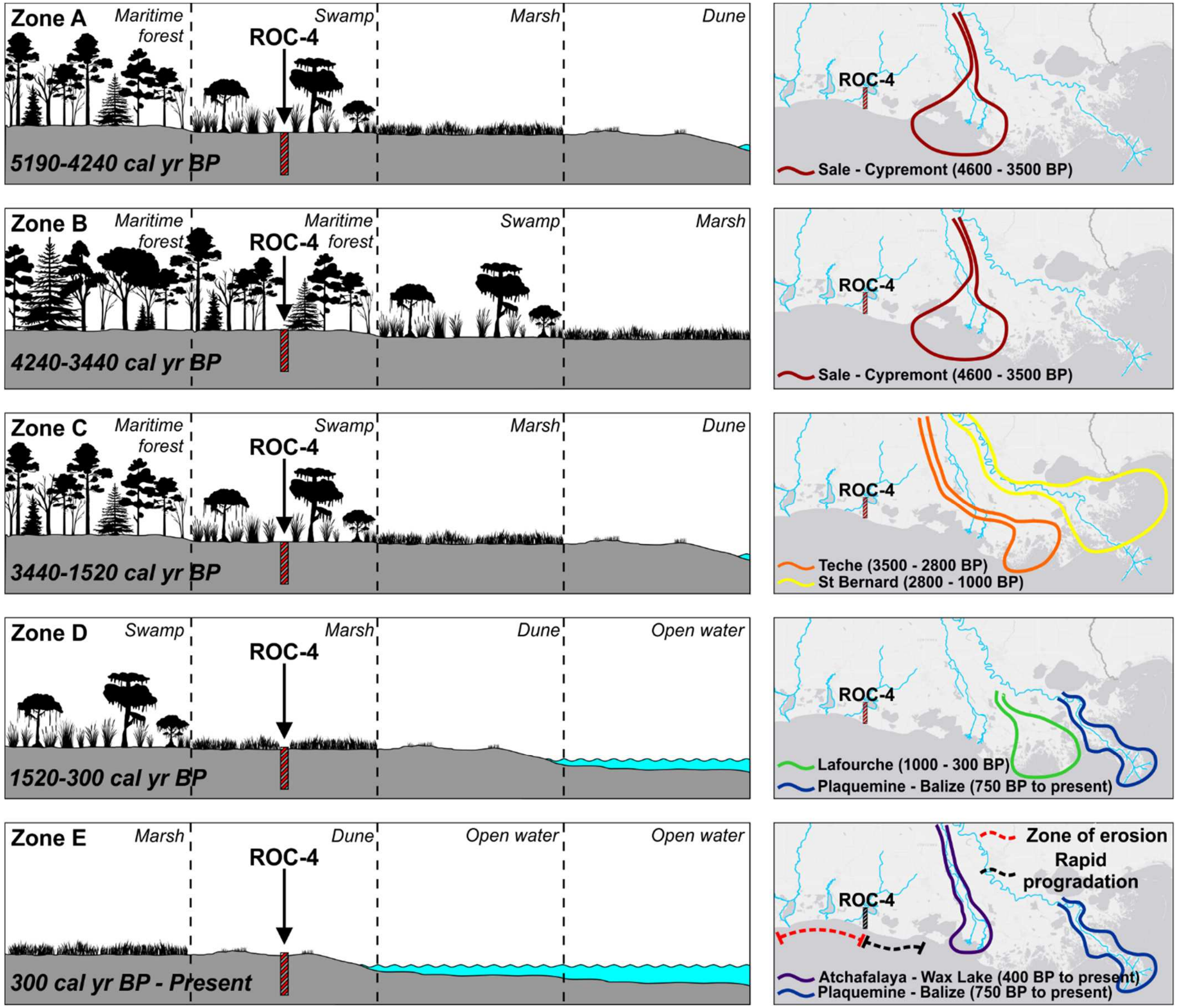

748

Figure 5

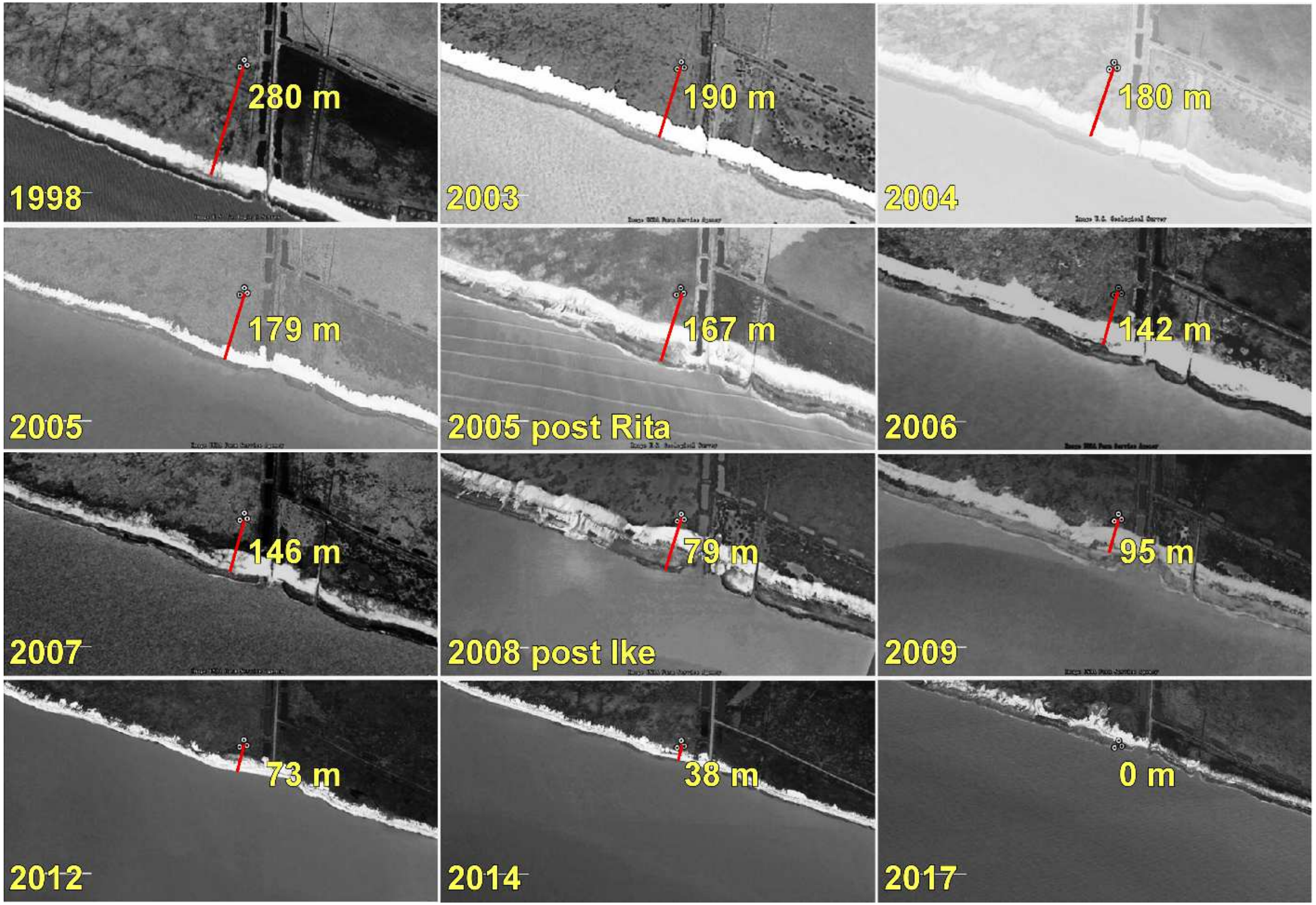
280 m
1998
190 m
2003
180 m
2004
179 m
2005
167 m
2005 post Rita
142 m
2006
146 m
2007
79 m
2008 post Ike
95 m
2009
73 m
2012
38 m
2014
0 m
2017

Table 1

Sample depth	Sediment type	Conventional age	Calibrated age (cal yr BP)	2-sigma calibration (cal yr BP)
78 cm	Organic sediment	580 +/- 30 BP	590	533 – 569 (0.333 %)
				582 – 649 (0.667 %)
403 cm	Organic sediment	3900 +/- 30 BP	4340	4247 – 4418 (100 %)
525 cm	Organic sediment	4530 +/- 30 BP	5190	5053 – 5190 (0.663 %)
				5214 – 5309 (0.337 %)

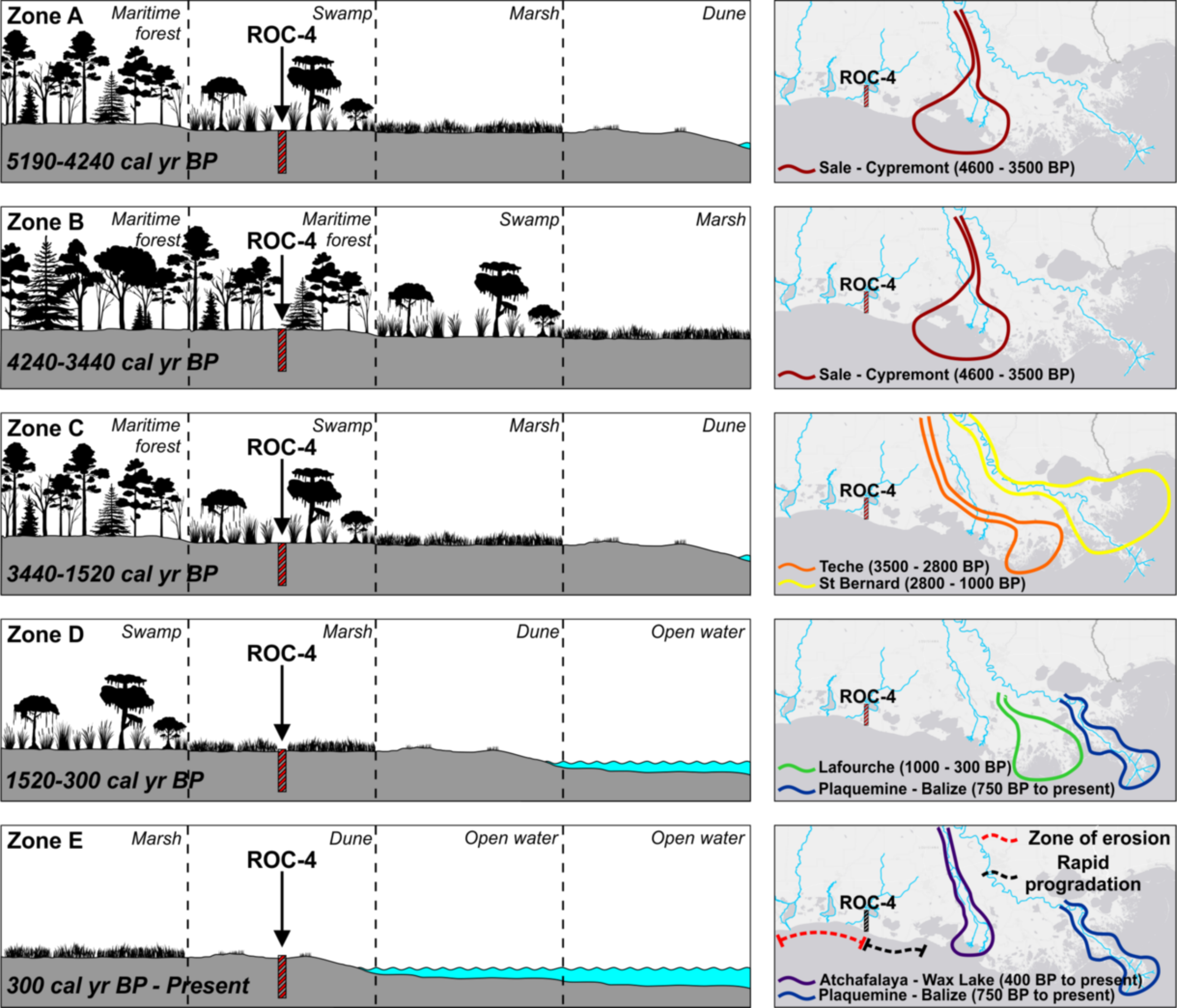

Zone A
Maritime forest
Swamp
Marsh
Dune
ROC-4
5190-4240 cal yr BP
ROC-4
Sale - Cypremont (4600 - 3500 BP)
Zone B
Maritime forest
Maritime forest
Swamp
Marsh
ROC-4
4240-3440 cal yr BP
ROC-4
Sale - Cypremont (4600 - 3500 BP)
Zone C
Maritime forest
Swamp
Marsh
Dune
ROC-4
3440-1520 cal yr BP
ROC-4
Teche (3500 - 2800 BP)
St Bernard (2800 - 1000 BP)
Zone D
Swamp
Marsh
Dune
Open water
ROC-4
1520-300 cal yr BP
ROC-4
Lafourche (1000 - 300 BP)
Plaquemine - Balize (750 BP to present)
Zone E
Marsh
Dune
Open water
Open water
ROC-4
300 cal yr BP - Present
Zone of erosion
Rapid progradation
ROC-4
Atchafalaya - Wax Lake (400 BP to present)
Plaquemine - Balize (750 BP to present)